



Preliminary communication

## Novel promising linezolid analogues: Rational design, synthesis and biological evaluation



Margherita De Rosa<sup>a</sup>, Anna Zanfardino<sup>c</sup>, Eugenio Notomista<sup>c</sup>, Thomas A. Wichelhaus<sup>d</sup>, Carmela Saturnino<sup>b, \*\*</sup>, Mario Varcamonti<sup>c, \*\*</sup>, Annunziata Soriente<sup>a, \*</sup>

<sup>a</sup> Dipartimento di Chimica e Biologia, Università degli Studi di Salerno, via Giovanni Paolo II, 132, 84084 Fisciano, SA, Italy

<sup>b</sup> Dipartimento di Farmacia, Università degli Studi di Salerno, via Giovanni Paolo II, 132, 84084 Fisciano, SA, Italy

<sup>c</sup> Dipartimento di Biologia, Università degli Studi di Napoli Federico II, Complesso Universitario Monte S. Angelo, Via Cinthia, 80126 Napoli, Italy

<sup>d</sup> Institute of Medical Microbiology and Infection Control, Hospital of Goethe-University, Paul-Ehrlich-Str. 40, 60596 Frankfurt/Main, Germany

### ARTICLE INFO

#### Article history:

Received 6 June 2013

Received in revised form

12 September 2013

Accepted 14 September 2013

Available online 25 September 2013

#### Keywords:

Linezolid

Oxazolidinone

Thiourea

Antibacterial

Structure–activity relationship

### ABSTRACT

A new series of 5-substituted oxazolidinones derived from linezolid, having urea and thiourea moieties at the C-5 side chain of the oxazolidinone ring, were prepared and their *in vitro* antibacterial activity was evaluated. The compound **10f** demonstrated high antimicrobial activity, comparable to that of linezolid against *Staphylococcus aureus*.

© 2013 Elsevier Masson SAS. All rights reserved.

## 1. Introduction

Today, the rising incidence of multidrug resistance in Gram-positive bacterial pathogens represents one of the most significant challenge for scientific communities worldwide highlighting the need for the search and discovery of new and more effective antibacterial agents. Linezolid (ZYVOX, Fig. 1) [1–3] is the only clinically used drug in the oxazolidinone class, a class of totally synthetic antibacterials, and has a broad spectrum of activity against Gram-positive bacteria [4–8]. It is highly effective for the treatment of serious infections caused by Gram-positive pathogens resistant to other antibiotics including methicillin-resistant *Staphylococcus aureus* (MRSA), vancomycin-resistant enterococci (VRE) and penicillin-resistant *Streptococcus pneumoniae*.

Significant to linezolid success are both favourable pharmacokinetic and toxic effect profiles consistent with oral or intravenous dosing in humans along with near-complete oral

bioavailability, and a number of characteristics appropriate to mitigate against the occurrence of drug resistance. In fact, linezolid is a completely synthetic drug; thus, no natural and pre-existing pool of resistance genes would be expected to favour the appearance of resistance mechanisms. Furthermore, it has a unique mechanism of action which targets bacterial ribosomal protein synthesis at an extremely early stage and consequently, cross-resistance between the drug and commercially available antimicrobials would be remote. Unfortunately, the emergence of linezolid-resistance in *S. aureus* and other bacteria has already been observed [9–11] highlighting once again the need for finding novel oxazolidinone-type drugs with improved potency, reduced toxicity and broader spectrum of activity. Studies into new oxazolidinones with different structural modifications and improved characteristic are ongoing and the research area is very active [6,12–16].

In this paper we describe the synthesis and antibacterial activity of previously unreported linezolid analogues bearing the urea and thiourea functionality at the C-5 position. We used a computational approach with the structure–activity relationship studies to gain insights into their design in order to find new derivatives with improved activity.

\* Corresponding author. Tel.: +39 (089)969584; fax: +39 (089)969663.

\*\* Corresponding authors.

E-mail address: [titti@unisa.it](mailto:titti@unisa.it) (A. Soriente).

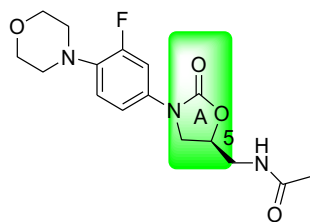


Fig. 1. Linezolid (Zyvox).

## 2. Results and discussion

### 2.1. Design and molecular modelling

Several research groups have tried to modify the four moieties of the linezolid molecule (Fig. 1) to obtain derivatives with improved activity on linezolid-resistant clinical strains. Different strategies have been used to select changes to linezolid structure including isosteric replacements, in particular in the case of rings A and C, and rational modelling based on the few available structures of ribosome–linezolid complexes. Two very recent examples are described in Refs. [17,18].

In order to design rationally linezolid derivatives with improved binding, particularly to ribosomes carrying mutations which confer partial or complete resistance to linezolid, we have selected as template the crystallographic structure of the 50S subunit of *Haloarcula marismortui* ribosome with linezolid and acetyl-phenylalanyl-CCA, an analogue of formyl-methionyl-tRNA (PDB code: 3CPW). The analysis of this complex suggested that the

oxazolidinone ring, the acetamide NH–CO, and the fluorophenyl ring make very close contacts with the ribosome and are essential to preserve the optimal conformation for binding, whereas, the acetamide methyl group and the morpholino ring make significantly less tight interactions. Moreover, the terminal methyl group points towards a wide solvent accessible cavity (Fig. 2A) lined by linezolid itself (the fluorophenyl moiety), the acetyl-phenylalanyl moiety and the nucleotides G2540, G2102, A2538, A2100, A2103 which are relatively close to the acetamidomethyl group. Other nucleotides, contributing to the cavity but slightly more distant from linezolid, are A2099, G2646, and U2541. As the mutations which confer resistance to linezolid increase the dimension and/or the flexibility of the binding pocket, thus reducing the ribosome/linezolid contacts, we planned to replace the acetyl moiety of linezolid with progressively larger groups in an attempt to compensate for the reduced steric complementarity. In a first phase several groups were appended to the nitrogen atom of linezolid and the resulting derivatives were manually docked into the pocket using linezolid in 3CPW as reference. These screening phase showed that substituted phenyl-(thio)ureas could fit well into the cavity described above. It is worth noting that linezolid derivatives bearing a 5-thiourea, 5-dithiocarbamate or 5-thiocarbamate group are effective antimicrobials [19–21]. Therefore, three phenyl-urea derivatives and the corresponding thiourea derivatives (Fig. 3) were selected to perform more accurate docking studies in the 50S subunit of *Haloarcula marismortui* ribosome using the bound linezolid molecule as template. However, as it is known that (di) substituted ureas and thioureas show a complex conformational behaviour [17–21], preliminary to the docking studies we have performed an accurate analysis of the six derivatives in the absence of the ribosome. Disubstituted (thio)urea derivatives can adopt the

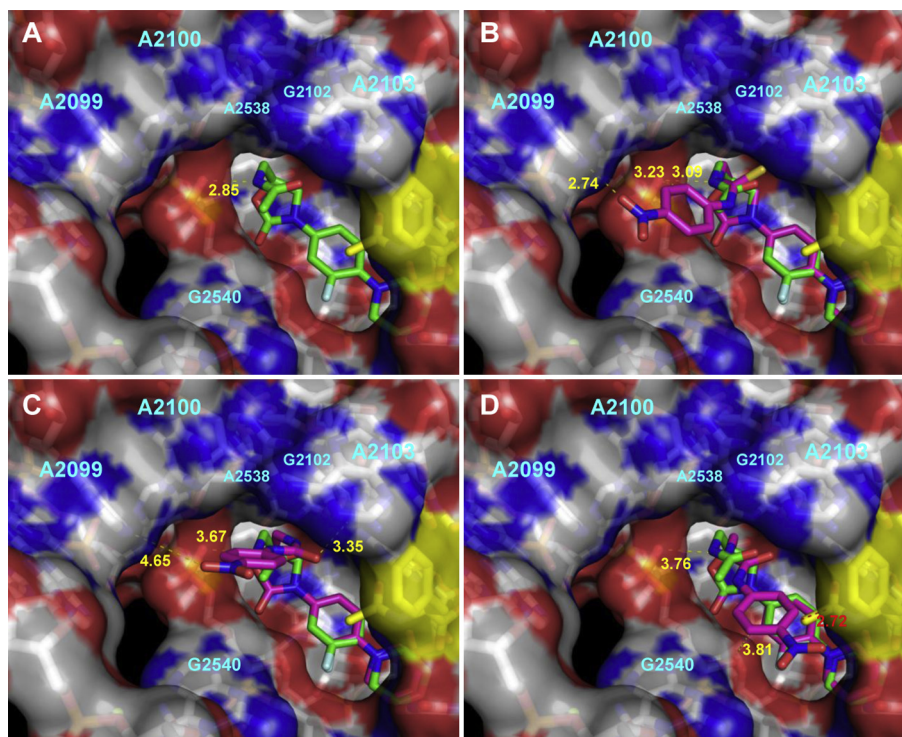


Fig. 2. Docking of linezolid (thio)urea derivatives into the linezolid binding site of *Haloarcula marismortui* ribosome (PDB code: 3CPW). Panel A shows the linezolid binding pocket solvent accessible surface. Panels B–D show, respectively, the docking of the syn–anti conformer of the *p*-nitro-phenyl-thiourea derivative, the anti–syn conformer and the syn–syn conformer of the *p*-nitro-phenyl-urea derivative. Nitrogen, oxygen and fluorine atoms are coloured blue, red and light cyan, respectively. Carbon atoms of ribosome, linezolid, linezolid derivatives and acetyl-phenylalanyl-CCA are coloured white, green, magenta and yellow, respectively. Yellow lines show potential H-bond or van der Waals contacts; distances are in Å. Red lines show distances lower than 3 Å. Labels are close to the N9 atoms of the corresponding nucleotides. (For interpretation of the references to colour in this figure legend, the reader is referred to the web version of this article.)

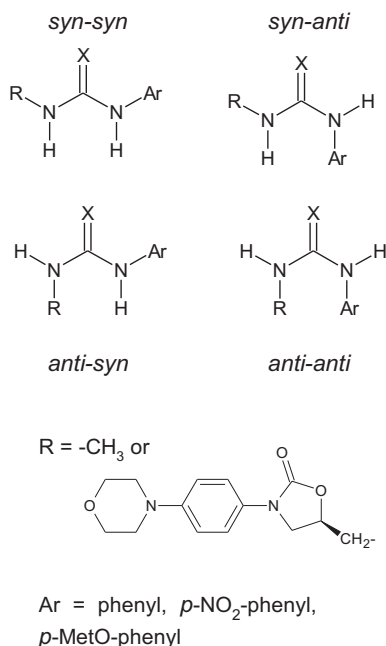


Fig. 3. Possible conformers of the 1-alkyl-3-aryl(thio)ureas studied in this paper.

four conformations shown in Fig. 3. The anti–anti conformer is strongly destabilized due to steric reasons, whereas, the stability of the remaining three conformations, according to literature, should depend on several factors including the presence of oxygen or sulphur, the nature of the substituents and the environment [22–26].

Unfortunately, the majority of the structural studies were done on crystals which introduce intermolecular constraints due, for example, to hydrogen bonding. For this reason we have modelled the compounds of Fig. 3 using two different strategies: the semi-empirical method AM1 was used to model 1-methyl-3-aryl(thio)ureas, whereas, the structures of the corresponding linezolid derivatives were modelled in water by using a molecular mechanics strategy (Monte Carlo minimization). The results are shown in Table 1 which reports the stability of the syn–anti and anti–syn conformers relatively to that of the syn–syn conformer.

Both methods suggest a noteworthy difference between ureas and thioureas as already discussed in several papers [22]. As for

thioureas, both AM1 and Monte Carlo methods suggest that the syn–anti conformer is the most stable, a result in agreement with several known structures of pure compounds [22,23] but also with the structure of several thiourea/protein complexes (e.g. ligand OM6 in PDB structure 2G8E; ligand URS in 1BUG; ligand PBD in 3PB7 and other six structures).

Fig. 4A shows the most stable conformation in water for the phenyl and the *p*-nitro-phenyl derivatives. It is worth noting that these compounds are able to adopt a “folded conformation” stabilized by a T shaped interaction between the two aromatic rings. The phenyl ring and the thiourea moiety are not coplanar as already observed in models and structures [22–24]. In the case of the urea derivatives it is more difficult to determine the most stable conformation for the lower  $\Delta E$  values. A recent study on the conformation of symmetric 1,3-dialkyl ureas has shown that the energy of the anti–syn/syn–anti conformer is only 0.5–0.7 kcal/mol higher than the syn–syn one [25]. On the contrary in the case of 1,3-diphenylurea the energy of the syn–syn conformer was found to be about 2 kcal/mol higher than the anti–syn/syn–anti one [26,27]. Given the small  $\Delta E$  values it is reasonable to expect that environmental and conformational effect can influence the rotation along the C–N bonds. Likely this could explain the disagreement between the AM1 and Monte Carlo methods. According to the

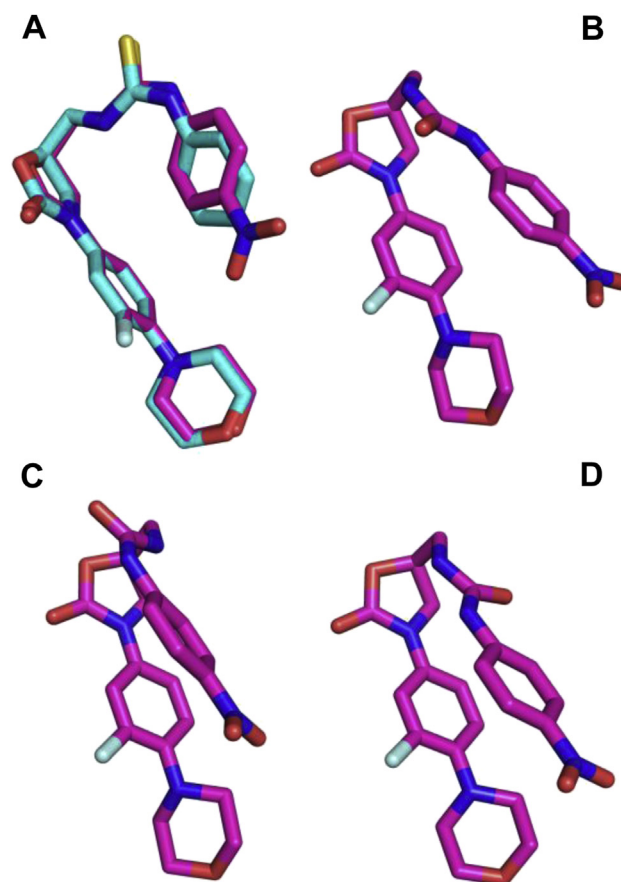


Fig. 4. Monte Carlo minimized models of the (thio)urea linezolid derivatives. Panel A shows the syn–anti conformer of the phenyl and the *p*-nitro-phenyl-thiourea derivatives. Panels B–D show, respectively, the models of the anti–syn, the syn–anti and the syn–syn conformers of the *p*-nitro-phenyl-urea derivative. Nitrogen, oxygen, carbon and fluorine atoms are coloured blue, red, magenta and light cyan, respectively. Carbon atoms of phenyl-thiourea derivative are coloured cyan. (For interpretation of the references to colour in this figure legend, the reader is referred to the web version of this article.)

**Table 1**  
Stability of the syn–anti and anti–syn conformers of (thio)urea derivatives of linezolid relatively to that of the syn–syn conformer.

Groups	R- <sup>a</sup>	Ar-	$\Delta E$			
			AM1		Monte Carlo	
			Urea	Thiourea	Urea	Thiourea
Met-/linezolid		<i>NO</i> <sub>2</sub> -Phe-				
		syn	–0.99	–2.26	–1.44	–2.08
anti		anti	–0.39	–3.59	0.35	–3.14
Met-/linezolid		Phe-				
		syn	–1.30	–2.46	–1.66	–2.44
anti		anti	–2.15	–5.25	0.87	–3.85
Met-/linezolid		MetO-Phe-				
		syn	–0.95	–2.37	n.d.	n.d.
anti		anti	–1.82	–4.72	n.d.	n.d.

<sup>a</sup> R- was a methyl group in the case of the AM1 analysis and linezolid in the case of the Monte Carlo analysis.

Monte Carlo method the anti-syn conformer is the most stable followed by the syn-syn one.

Fig. 4B–D shows the three possible conformers of *p*-nitro-phenyl-urea derivative modelled in water. The corresponding conformers of the phenyl-urea derivative adopt similar “folded conformations”. It is interesting to note that the conformations of the urea derivatives, unlike the thiourea derivatives, are characterized by stacking interactions between the aromatic rings. Finally, several known structures of 1-alkyl-3-aryl-urea/protein complexes in PDB database show the syn-syn conformation but in the majority of these complexes the two NH groups make hydrogen bonds with the same or two adjacent CO groups in the protein (e.g. ligand OHD in PDB structure 3V8S; ligand OQJ in 4EKG; ligand AW0 in 4EQZ; ligand BDQ in 3L5C). On the basis of the energy calculations and the available experimental structures, the syn-syn and the anti-syn conformers, likely, are the most stable conformers of the aryl-urea derivatives of linezolid.

The syn-syn, the anti-syn and the syn-anti conformers were docked in the linezolid pocket of 3CPW (Fig. 2B–D). The syn-anti conformer of the *p*-nitro-phenyl-thiourea derivative fits particularly well the cavity (Fig. 2B): the first NH of the thiourea moiety is still at hydrogen bond distance from the oxygen of the phosphate of G2540 (about 3.1 Å versus 2.85 Å in the case of linezolid); the nitro-phenyl moiety makes Van der Waals contacts with the phosphate and the ribose of G2540; the oxygen of the nitro group is at hydrogen bonding distance from the N6 of the adenine moiety of A2099; one of the aromatic CH in meta to the NO<sub>2</sub> group is at about 3.2 Å from the oxygen of the phosphate of G2540 thus making favourable electrostatic interactions (according to AM1 the partial charge on this hydrogen is 0.164).

The anti-syn conformer of the *p*-nitro-phenyl-urea derivative fits less well (Fig. 2C) as the anti conformation at the –CH<sub>2</sub>–NH– prevent the formation of the hydrogen bond with the phosphate of

G2540, the nitro group is too far from the N6 of the adenine moiety of A2099 to form a hydrogen bond, the nitro-phenyl moiety makes less tight Van der Waals contacts with the phosphate and the ribose of G2540.

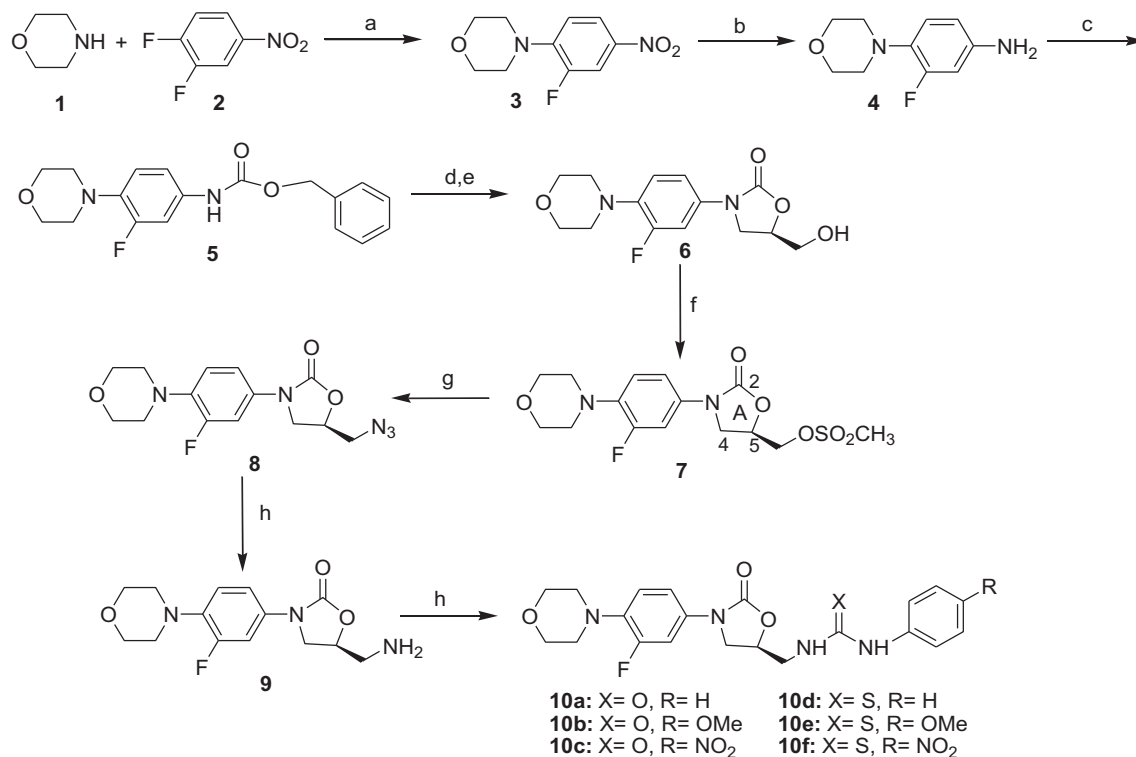
The syn-syn conformer of the *p*-nitro-phenyl-urea derivative (Fig. 2D) is still able to make the hydrogen bond with the phosphate of G2540 but the nitro-phenyl moiety makes prevalently intramolecular interactions maintaining a conformation similar to that adopted in water. Van der Waals contacts are formed with the ribose of G2540, but the phenyl ring is too close to the acetyl moiety of acetyl-phenylalanyl-CCA.

On the basis of these findings we decided to synthesize the three aryl-urea derivatives **10a–c** and the corresponding thiourea derivatives **10d–f**.

## 2.2. Chemistry

The synthetic route to the target compounds **10a–f** is shown in Scheme 1. They were prepared from key intermediate **7** synthesized starting from commercially available morpholine **1** and 3,4-difluoronitrobenzene **2** in good yield according to published procedure (Scheme 1) [1].

The formation of oxazolidinone ring with defined stereochemistry at the A-ring C-5 position was accomplished using *n*-butyllithium and (*R*)-(-)-glycidyl butyrate [1]. Derivatization of the alcohol **6** to the mesylate **7**, followed by nucleophilic displacement of the mesyl group in the presence of NaN<sub>3</sub> in DMF gave the azide **8**. Hydrogenation of the azide **8** over Pd/C (10%) in ethyl acetate at room temperature afforded the amino derivative **9** in quantitative yield [2]. Compound **9** was reacted with a range of different iso(-thio)cyanate reagents to give the target compounds **10a–f** in high yield. All the reported compounds were characterized by analytical spectroscopic methods (<sup>1</sup>H and <sup>13</sup>C NMR, MS) and elemental analysis.



**Scheme 1.** Synthesis of 5-substituted oxazolidinone derivatives. Reagents and conditions: (a) *i*-Pr<sub>2</sub>EtN, AcOEt; (b) HCO<sub>2</sub>NH<sub>4</sub>, 10% Pd/C, THF/MeOH; (c) benzyl chloroformate, NaHCO<sub>3</sub>, acetone/H<sub>2</sub>O; (d) *n*-BuLi, THF, –78 °C; (e) (*R*)-(-)-glycidyl butyrate, –78 °C-rt; (f) MsCl, Et<sub>3</sub>N, CH<sub>2</sub>Cl<sub>2</sub>; (g) NaN<sub>3</sub>, DMF, 70 °C; (h) 10% Pd/C, H<sub>2</sub>, AcOEt; (i) RPhNCX, CH<sub>2</sub>Cl<sub>2</sub>, rt.

### 2.3. Antimicrobial activity of linezolid analogues

The antimicrobial activities of the various linezolid analogues, all belonging to the class of oxazolidinones, were tested against *S. aureus*.

Minimal inhibitory concentrations (MICs) were determined for all linezolid analogues, i.e. compounds **10a–f**, against methicillin-susceptible *S. aureus* ATCC 29213. **10a–c** and **10e** showed a MIC higher than 100 µg/mL, instead **10d** was able to inhibit the *S. aureus* ATCC 29213 at a concentration of 10 µg/mL. Finally **10f** was the most active compound having a MIC of 2 µg/mL comparable to the activity of linezolid (Table 2). These findings are in agreement with the results of the molecular modelling analysis of linezolid derivatives which suggests that urea and thiourea derivatives should bind to the ribosome with very different orientations. The higher activity of **10f** with respect to **10d** could be likely attributed to the additional interactions between the –NO<sub>2</sub> group and the purine ring of A2099. At the moment it is less clear why **10e** is not active. A possible explanation is that the methoxy moiety of **10e** is not able to make the hydrogen bond with the N6 of A2099 and also is too close to the purine ring. Moreover, other features of **10e** like, for example, impaired penetration into the cells, could contribute to decrease the antimicrobial efficacy. More accurate analysis will be necessary to address these aspects.

As **10f** was considered the most promising candidate for further studies, we tested this linezolid analogue also against methicillin-resistant *S. aureus* ATCC 43300 (Table 3).

The experimental data indicate that **10f** shows similar activity compared to linezolid against methicillin-susceptible and methicillin-resistant *S. aureus*. After this important result, our studies will be directed to the analysis of **10f** activity against some linezolid-resistant strains and to the comprehension of **10f** mechanism of action.

### 3. Conclusion

In summary, a series of novel linezolid analogues has been designed, prepared and tested for antibacterial activity. The approach based on molecular modelling has been useful and profitable for the realization of an analogue (**10f**) that we have shown to be highly active against methicillin-susceptible and methicillin-resistant *S. aureus*. This result is very promising for the design of further studies directed against strains of *S. aureus* resistant to linezolid and to achieve new analogues starting from **10f**.

### 4. Experimental section

#### 4.1. Molecular modelling

The ZMM-MVM molecular modelling package (ZMM Software Inc.; <http://www.zmmsoft.com>) was used for the conformational

**Table 2**  
MICs of linezolid and linezolid analogues against *S. aureus* ATCC 29213.

Compound	MIC <sup>a</sup> (µg/mL)
<b>10a</b>	>100
<b>10b</b>	>100
<b>10c</b>	>100
<b>10e</b>	>100
<b>10d</b>	10
<b>10f</b>	2
Linezolid	1

<sup>a</sup> MICs present the median of three experiments.

**Table 3**  
MICs of linezolid and **10f** against *S. aureus* ATCC 29213 and *S. aureus* ATCC 43300.

	MIC <sup>a</sup> (µg/mL)	
	Linezolid	<b>10f</b>
<i>S. aureus</i> ATCC 29213	1	2
<i>S. aureus</i> ATCC 43300	1	1

<sup>a</sup> MICs present the median of three experiments.

analysis of linezolid derivatives in water [28]. Atom–atom interactions were calculated using the AMBER force field with a cutoff distance of 8 Å. Conformational energy calculations included van der Waals, electrostatic, H-bonds, torsion components and hydration component [29]. Electrostatic interactions were calculated with an environment- and distance-dependent relative dielectric constant. Linezolid derivatives were prepared using the PyMOL software (DeLano Scientific LLC). Geometry was optimized using the “ZI” module of ZMM. Partial charges were attributed using the AM1 method in the HyperChem software (HyperCube Inc., <http://www.hyper.com>). Optimized derivatives were manually docked into the linezolid binding site of ribosome structure (3CPW) using the PyMOL software. The HyperChem software was also used to model 1-methyl-3-aryl(thio)ureas.

#### 4.2. Chemistry. General methods

All reagents and anhydrous solvents were obtained from commercial sources and used without further purification. All reactions requiring anhydrous conditions were performed under N<sub>2</sub> atmosphere and all glassware were flame dried. Elemental analyses were performed on the FlashEA 1112 Series with Thermal Conductivity Detector (Thermo Electron Corporation). <sup>1</sup>H and <sup>13</sup>C NMR spectra were recorded on a Bruker AM 250 (250.13 MHz for <sup>1</sup>H, 62.89 MHz for <sup>13</sup>C), Bruker DRX 300 (300 MHz for <sup>1</sup>H; 75 MHz for <sup>13</sup>C) and Bruker DRX 400 (400 MHz for <sup>1</sup>H; 100 MHz for <sup>13</sup>C). *J* values are given in Hz. The <sup>1</sup>H chemical shifts were referenced to the solvent peak: CDCl<sub>3</sub> (7.26 ppm), and the <sup>13</sup>C chemical shifts were referenced to the solvent peak: CDCl<sub>3</sub> (77.0 ppm). Mass spectra were recorded on a Micromass Quattro micro API mass spectrometer (EI, 70 eV). IR spectra were recorded on an FT-IR instrument (Bruker Vector 22). Melting points were performed on DSC 2920 TA Instruments. Thin-layer chromatography was performed on Macherey–Nagel pre-coated aluminium sheets (0.20 mm, silica gel 60 with fluorescent indicator UV<sub>254</sub>) in appropriate solvent. Column chromatography was carried out using silica gel 60 (70–230 mesh ASTM, Merck).

Compounds **3–8** were prepared according to the previously described procedure [1] and their spectral features matched with those reported in literature.

##### 4.2.1. (*S*)-5-(aminomethyl)-3-(3-fluoro-4-morpholinophenyl)oxazolidin-2-one (**9**)

To a solution of azide **8** (140 mg, 0.44 mmol) in ethyl acetate (16.5 mL) 10% Pd(C) (16.5 mg) were added. The reaction was carried out under H<sub>2</sub> balloon condition and was vigorously stirred at room temperature overnight. The solution was filtered through a plug of diatomaceous earth and concentrated under reduced pressure to afford the title compound as white solid (137 mg) which was used without purification. <sup>1</sup>H NMR (CDCl<sub>3</sub>, 250 MHz): δ 7.45 (dd, 1H, *J* = 2.35 Hz, 14.5 Hz), 7.13–7.10 (m, 1H), 6.91 (t, 1H, *J* = 9.2 Hz), 4.71–4.61 (m, 1H), 4.00 (t, 1H, *J* = 8.7 Hz), 3.87–3.77 (m, 5H), 3.14–2.87 (m, 6H), 1.7 (bs, 2H). <sup>13</sup>C NMR (CDCl<sub>3</sub>, 62.89 MHz): δ 155.2 (d, *J* = 245.84 Hz), 154.4, 136.0 (d, *J* = 8.9 Hz), 133.1 (d, *J* = 10.5 Hz), 118.6 (d, *J* = 4.1 Hz), 113.5, 107.1 (d, *J* = 26.2 Hz), 73.6, 66.7, 50.8, 47.4,

44.6. IR (KBr pellet,  $\text{cm}^{-1}$ ):  $\nu$  3401, 2952, 1726, 1225. MS:  $m/z$  295 ( $\text{M}^+$ ).

#### 4.2.2. Synthesis of **10a–f** compounds. General method

In a round bottom flask equipped with a stir bar, to a solution of **9** (21 mg, 0.07 mmol) in dry  $\text{CH}_2\text{Cl}_2$  (1.61 mL) the appropriate iso (thio)cyanate was added. The reaction was stirred at room temperature overnight. The solvent was removed under reduced pressure and the resulting residue was purified by flash chromatography ( $\text{CH}_2\text{Cl}_2/\text{MeOH}$ ) followed by preparative thin-layer chromatography to give the pure final compounds.

4.2.2.1. 1-(((S)-3-(3-fluoro-4-morpholinophenyl)-2-oxooxazolidin-5-yl)methyl)-3-phenylurea (**10a**). Purification by silica gel column chromatography ( $\text{CH}_2\text{Cl}_2/\text{MeOH}$  95/5) gave a white solid (90% yield), m.p. 218–222 °C.  $[\alpha]_D^{20}$  –18° (c 0.67, DMSO)  $^1\text{H}$  NMR ( $\text{CDCl}_3$ , 400 MHz):  $\delta$  7.46 (dd, 1H,  $J$  = 2.60 Hz, 15.0 Hz), 7.32–7.26 (m, 5H), 7.13–7.06 (m, 1H), 7.05–6.94 (m, 2H), 5.75 (bs, 1H), 4.93–4.81 (m, 1H), 4.08 (t, 1H,  $J$  = 8.8 Hz), 3.99–3.88 (m, 5H), 3.84–3.57 (m, 2H), 3.19–3.05 (m, 4H).  $^{13}\text{C}$  NMR ( $\text{CDCl}_3$ , 100.03 MHz):  $\delta$  156.0, 155.4 (d,  $J$  = 246.10 Hz), 154.9, 138.4 (x2), 129.1 (x2), 123.6 (x2), 122.30, 120.3 (x2), 114.2, 108.0 (d,  $J$  = 26.0 Hz), 72.8, 66.5 (x2), 51.2 (x2), 47.4, 42.1. IR (KBr pellet,  $\text{cm}^{-1}$ ):  $\nu$  3475, 2970, 1736, 1569, 1385. MS:  $m/z$  414 ( $\text{M}^+$ ), 437 ( $\text{M} + \text{Na}$ ) $^+$ . Anal Calcd for  $\text{C}_{21}\text{H}_{23}\text{N}_4\text{O}_4\text{F}$ : C: 60.86, H: 5.59, N: 13.52. Found C: 60.88, H: 5.56, N 13.46.

4.2.2.2. 1-(((S)-3-(3-fluoro-4-morpholinophenyl)-2-oxooxazolidin-5-yl)methyl)-3-(4-methoxyphenyl)urea (**10b**). Purification by silica gel column chromatography ( $\text{CH}_2\text{Cl}_2/\text{MeOH}$  99/1) gave a white solid (95% yield), m.p. 198–201 °C.  $[\alpha]_D^{20}$  –25° (c 0.98, DMSO)  $^1\text{H}$  NMR ( $\text{CDCl}_3$ , 300 MHz):  $\delta$  7.55 (dd, 1H,  $J$  = 2.6 Hz, 14.3 Hz), 7.14–7.07 (m, 3H), 6.95–6.86 (m, 3H), 5.28 (bs, 1H), 4.80–4.78 (m, 1H), 4.02 (t, 1H,  $J$  = 8.9 Hz), 3.92–3.86 (m, 5H), 3.81 (s, 3H), 3.69–3.65 (m, 2H), 3.07–3.04 (m, 4H).  $^{13}\text{C}$  NMR ( $\text{CDCl}_3$ , 100.03 MHz):  $\delta$  155.3, 154.3 (d,  $J$  = 246.10 Hz), 147.2 (x2), 141.0 (x2), 136.2, 134.0, 125.5 (x2), 119.9, 117.4 (x2), 114.5, 106.8 (d,  $J$  = 31.9 Hz), 72.0, 66.3 (x2), 50.8 (x2), 47.3, 42.0. IR (KBr pellet,  $\text{cm}^{-1}$ ):  $\nu$  3381, 3301, 2950, 1739, 1675, 1634, 1559, 1511, 1244. MS:  $m/z$  467 ( $\text{M} + \text{Na}$ ) $^+$ . Anal Calcd for  $\text{C}_{22}\text{H}_{25}\text{N}_4\text{O}_5\text{F}$ : C: 59.45, H: 5.67, N: 12.61. Found C: 59.50, H: 5.64, N 12.65.

4.2.2.3. 1-(((S)-3-(3-fluoro-4-morpholinophenyl)-2-oxooxazolidin-5-yl)methyl)-3-(4-nitro-phenyl)urea (**10c**). Purification by silica gel column chromatography ( $\text{CH}_2\text{Cl}_2/\text{MeOH}$  95/5) gave a yellow solid (90% yield), m.p. 245–248 °C.  $[\alpha]_D^{20}$  –22° (c 0.67, DMSO)  $^1\text{H}$  NMR (DMSO, 300 MHz):  $\delta$  9.40 (bs, 1H), 8.13 (d, 2H,  $J$  = 12.2 Hz), 7.61 (d, 2H,  $J$  = 12.2 Hz), 7.50 (dd, 1H,  $J$  = 2.6 Hz, 14.3 Hz), 7.20–7.17 (m, 1H), 7.07–7.01 (m, 2H), 4.88–4.75 (m, 1H), 4.11 (t, 1H,  $J$  = 9.1 Hz), 3.85–3.72 (m, 5 H), 3.49–3.35 (m, 2H), 2.91–2.94 (m, 4H).  $^{13}\text{C}$  NMR (DMSO, 75.5 MHz):  $\delta$  155.3, 155.2, 154.2, 150.7 (d,  $J$  = 246.10 Hz), 132.0, 130.7, 129.1, 123.8 (x2), 119.1, 114.5, 114.2 (x2), 107.7 (d,  $J$  = 26.0 Hz), 72.7, 66.8 (x2), 55.5, 51.1 (x2), 47.5, 42.4. IR (KBr pellet,  $\text{cm}^{-1}$ ):  $\nu$  3315, 2960, 1745, 1518, 1381. MS:  $m/z$  460 ( $\text{M} + 1$ ) $^+$ . Anal Calcd for  $\text{C}_{21}\text{H}_{22}\text{N}_5\text{O}_6\text{F}$ : C: 54.90, H: 4.83, N: 15.24. Found C: 54.78, H: 4.81, N: 15.28.

4.2.2.4. 1-(((S)-3-(3-fluoro-4-morpholinophenyl)-2-oxooxazolidin-5-yl)methyl)-3-phenyl thiourea (**10d**). Purification by silica gel column chromatography ( $\text{CH}_2\text{Cl}_2/\text{MeOH}$  99/1) gave a white solid (86% yield), m.p. 163–166 °C.  $[\alpha]_D^{20}$  –26° (c 0.95, DMSO)  $^1\text{H}$  NMR (DMSO, 250 MHz):  $\delta$  9.75 (bs, 1H), 8.05 (bs, 1H), 7.52 (dd, 1H,  $J$  = 2.3 Hz, 14.8 Hz), 7.40–7.30 (m, 5H), 7.23–7.19 (m, 1H), 7.15–7.03 (m, 1H), 4.96–4.88 (m, 1H), 4.13 (t, 1H,  $J$  = 9.2 Hz), 3.90–3.84 (m, 2H), 3.75–3.71 (m, 4H), 3.40–3.34 (m, 1H), 2.94–2.97 (m, 4H).  $^{13}\text{C}$  NMR (DMSO, 75.5 MHz):  $\delta$  182.0, 154.9 (d,  $J$  = 243.9 Hz), 154.4, 139.3,

136.0, 135.9, 129.1 (x2), 124.8 (x2), 123.7, 119.7, 114.6, 107.1 (d,  $J$  = 26.1 Hz), 71.6, 66.5 (x2), 51.1 (x2), 47.5, 46.8. IR (KBr pellet,  $\text{cm}^{-1}$ ):  $\nu$  3343, 2980, 1736, 1591, 1385. MS:  $m/z$  430 ( $\text{M}^+$ ). Anal Calcd for  $\text{C}_{21}\text{H}_{23}\text{F N}_4\text{O}_3\text{S}$ : C: 58.59, H: 5.39, N: 13.01. Found C: 58.79, H: 5.34, N: 12.97.

4.2.2.5. 1-(((S)-3-(3-fluoro-4-morpholinophenyl)-2-oxooxazolidin-5-yl)methyl)-3-(4-methoxyphenyl)thiourea (**10e**). Purification by silica gel column chromatography ( $\text{CH}_2\text{Cl}_2/\text{MeOH}$  95/5) gave a white solid (90% yield), m.p. 150–152 °C.  $[\alpha]_D^{20}$  –30° (c 0.93, DMSO)  $^1\text{H}$  NMR (DMSO, 250 MHz):  $\delta$  9.60 (bs, 1H), 7.87 (bs, 1H), 7.50 (dd, 1H,  $J$  = 2.1 Hz, 14.8 Hz), 7.22–7.19 (m, 3H), 7.07 (t, 1H,  $J$  = 9.5 Hz), 6.88 (d, 2H,  $J$  = 8.7 Hz), 4.94–4.88 (m, 1H), 4.11 (t, 1H,  $J$  = 9.0 Hz), 3.90–3.87 (m, 2H), 3.75–3.72 (m, 7H), 2.98–2.94 (m, 5H).  $^{13}\text{C}$  NMR (DMSO, 75.5 MHz):  $\delta$  182.0, 156.9, 154.5 (d,  $J$  = 243.9 Hz), 154.2, 135.7 (d,  $J$  = 8 Hz), 133.4, 131.0, 126.2 (x2), 119.4, 114.4, 114.1 (x2), 106.9 (d,  $J$  = 26 Hz), 71.4, 66.3 (x2), 55.4, 50.8 (x2), 47.3, 46.7. IR (KBr pellet,  $\text{cm}^{-1}$ ):  $\nu$  3362, 2995, 1743, 1375. MS:  $m/z$  483 ( $\text{M} + \text{Na}$ ) $^+$ . Anal Calcd for  $\text{C}_{22}\text{H}_{25}\text{F N}_4\text{O}_4\text{S}$ : C: 57.38, H: 5.47, N: 12.17. Found C: 57.25, H: 5.49, N: 12.15.

4.2.2.6. 1-(((S)-3-(3-fluoro-4-morpholinophenyl)-2-oxooxazolidin-5-yl)methyl)-3-(4-nitro-phenyl)thiourea (**10f**). Purification by silica gel column chromatography ( $\text{CH}_2\text{Cl}_2/\text{MeOH}$  95/5) gave a yellow solid (90% yield), m.p. 190–193 °C.  $[\alpha]_D^{20}$  –23° (c 0.95, DMSO)  $^1\text{H}$  NMR (DMSO, 300 MHz):  $\delta$  10.30 (bs, 1H), 8.55 (bs, 1H), 8.17 (d, 2H,  $J$  = 9.2 Hz), 7.82 (d, 2H,  $J$  = 9.2 Hz), 7.51 (dd, 1H,  $J$  = 2.3 Hz, 14.8 Hz), 7.23–7.20 (m, 1H), 7.07 (t, 1H,  $J$  = 9.6 Hz), 5.01–4.93 (m, 1H), 4.15 (t, 1H,  $J$  = 9.0 Hz), 3.94–3.90 (m, 1H), 3.87–3.81 (m, 1H), 3.74–3.71 (m, 4H), 2.97–2.94 (m, 5H).  $^{13}\text{C}$  NMR (DMSO, 62.89 MHz):  $\delta$  181.0, 154.7 (d,  $J$  = 243.9 Hz), 154.0, 146.0, 142.4, 135.6, 133.3, 124.5 (x2), 120.9 (x2), 119.3, 114.2, 106.7 (d,  $J$  = 27 Hz), 71.0, 66.2 (x2), 50.7 (x2), 47.2, 46.4. IR (KBr pellet,  $\text{cm}^{-1}$ ):  $\nu$  3346, 3104, 1752, 1516, 1328. MS:  $m/z$  475 ( $\text{M}^+$ ). Anal Calcd for  $\text{C}_{21}\text{H}_{22}\text{FN}_5\text{O}_5\text{S}$ : C: 53.04, H: 4.66, N: 14.73. Found C: 53.10, H: 4.65, N: 14.76.

#### 4.3. Minimum inhibitory concentration (MIC) determination

Minimal inhibitory concentrations (MICs) of linezolid and its various analogues were determined according to microdilution method established by Clinical and Laboratory Standards Institute (CLSI). Therefore, 95  $\mu\text{L}$  of cation-adjusted Mueller-Hinton broth supplemented with the different compounds at various concentrations ranging from 128 to 0.06  $\mu\text{g}/\text{mL}$  were added to each well of a 96-well microtiter plate. Five microlitres of a bacterial suspension were added to each well to yield a final concentration of about  $5 \times 10^5$  cells/mL. MICs were determined after 16–20 h of incubation at  $35 \pm 2$  °C. National Committee for Clinical Laboratory Standards. Performance standards for antimicrobial susceptibility testing; Ninth informational supplement. NCCLS document M100-S9 [ISBN1-56238-358-2]. NCCLS, 940 West Valley Road, Wayne, Pa19087-1898 USA, 1999. Ref.

#### Acknowledgements

We are grateful for the financial support from the Ministero dell'Istruzione, dell'Università e della Ricerca (MIUR). Our thanks to Dr. Ivano Immediata for experimental support in the characterization of new compounds.

#### References

- [1] K.L. Leach, S.J. Brickner, M.C. Noe, P.F. Miller, *Ann. N. Y. Acad. Sci.* 1222 (2011) 49–54.

- [2] C.W. Ford, G.E. Zurenko, M.R. Barbachyn, *Curr. Drug Targets Infect. Dis.* 1 (2001) 181–199.
- [3] S.J. Brickner, M.R. Barbachyn, D.K. Hutchinson, P.R. Manninen, *J. Med. Chem.* 51 (2008) 1981–1990.
- [4] D.K. Hutchinson, *Antimicrob. Agents Chemother.* 41 (1997) 2132–2136.
- [5] D.J. Diekema, R.N. Jones, *Lancet* 358 (2001) 1975–1982.
- [6] D.K. Hutchinson, *Curr. Top. Med. Chem.* 3 (2003) 1021–1042.
- [7] M.R. Barbachyn, C.W. Ford, *Angew. Chem. Int. Ed.* 42 (2003) 2010–2023.
- [8] B. Bozdogan, P.C. Appelbaum, *Int. J. Antimicrob. Agents* 23 (2004) 113–119.
- [9] V.G. Meka, H.S. Gold, *Clin. Infect. Dis.* 39 (2004) 1010–1015.
- [10] G. Morales, J.J. Picazo, E. Baos, F.J. Candel, A. Arribi, B. Peláez, R. Andrade, M.-A. de la Torre, J. Fereres, M. Sánchez-García, *Clin. Infect. Dis.* 50 (2010) 821–825.
- [11] K.S. Long, B. Vester, *Antimicrob. Agents Chemother.* 56 (2011) 603–612.
- [12] M.B. Gravestock, *Curr. Opin. Drug Discov. Devel.* 8 (4) (2005) 469–477.
- [13] A.R. Renslo, G.W. Luehr, M.F. Gordeev, *Bioorg. Med. Chem.* 14 (12) (2006) 4227–4240.
- [14] J.V.N.V. Prasad, *Curr. Opin. Microbiol.* 10 (2007) 454–460.
- [15] G. Poce, G. Zappia, G.C. Porretta, B. Botta, M. Biava, *Exp. Opin. Ther. Patents* 18 (2008) 97–121.
- [16] G. Pintér, I. Bereczki, E. Röth, A. Sipos, R. Varghese, E. Ekpenyong Udo, E. Ostorházi, F. Rozgonyi, O.A. Phillips, P. Herczegh, *Med. Chem.* 7 (2011) 45–55.
- [17] A. Palumbo Piccionello, R. Musumeci, C. Cocuzza, C.G. Fortuna, A. Guarcello, P. Pierro, A. Pace, *Eur. J. Med. Chem.* 50 (2012) 441–448.
- [18] C.G. Fortuna, C. Bonaccorso, A. Bulbarelli, G. Caltabiano, L. Rizzi, L. Goracci, G. Musumarra, A. Pace, A. Palumbo Piccionello, A. Guarcello, P. Pierro, C.E.A. Cocuzza, R. Musumeci, *Eur. J. Med. Chem.* 65 (2013) 533–545.
- [19] R. Tokuyama, Y. Takahashi, Y. Tomita, T. Suzuki, T. Yoshida, N. Iwasaki, N. Kado, E. Okezaki, O. Nagata, *Chem. Pharm. Bull.* 49 (4) (2001) 347–352.
- [20] R. Tokuyama, Y. Takahashi, Y. Tomita, M. Tsubouchi, T. Yoshida, N. Iwasaki, N. Kado, E. Okezaki, O. Nagata, *Chem. Pharm. Bull.* 49 (4) (2001) 353–360.
- [21] R. Tokuyama, Y. Takahashi, Y. Tomita, M. Tsubouchi, N. Iwasaki, N. Kado, E. Okezaki, O. Nagata, *Chem. Pharm. Bull.* 49 (4) (2001) 361–367.
- [22] K. Wozniak, I. Wawer, D. Stroehl, *J. Phys. Chem.* 99 (1995) 8888–8895 and references therein.
- [23] A. Saxena, R.D. Pike, *J. Chem. Crystallogr.* 37 (2007) 755–764.
- [24] V.S. Bryantsev, B.P. Hay, *J. Phys. Chem. A* 110 (2006) 4678–4688.
- [25] M. Obrzud, Maria Rospenk, Aleksander Koll, *J. Phys. Chem. B* 114 (2010) 15905–15912.
- [26] R. Emery, N.A. Macleod, L.C. Snoek, J.P. Simons, *Phys. Chem. Chem. Phys.* 6 (2004) 2816–2820.
- [27] S. Besier, A. Ludwig, J. Zander, V. Brade, T.A. Wichelhaus, *Antimicrob. Agents Chemother.* 52 (2008) 1570–1572.
- [28] B.S. Zhorov, P.D. Bregestovski, *Biophys. J.* 78 (2000) 1786–1803.
- [29] T. Lazaridis, M. Karplus, *Proteins* 35 (1999) 133–152.